$$r_m = sqrt\left((s - d_1)(s - d_2)(s - d_3)/s\right) \quad (13)$$

The equation of the inscribed circle is given as:

$$\left(x - x_m\right)^2 + \left(y - y_m\right)^2 = r_m^{\;2} \quad (14)$$

- A line is sketched through the latest two posit -ion of the target B_i (x_{i-1}, y_{i-1}) and B_{i+1} (x_i, y_i) which is $y = kx + c$, where k is the slope and c is the y-intercept which are computed as below:

$$k = \left(y_i - y_{i-1}\right) \,/\, \left(x_i - x_{i-1}\right) \quad (15)$$

$$c = \left(x_i y_{i-1} - x_{i-1} y_i\right)/\left(x_i - x_{i-1}\right) \quad (16)$$

Another circle is also drawn such that its radius 'r_n' is the half of the distance between the latest two position of the target B_i and B_{i+1} in the same directional movement of the target as shown in Figure 2. The equation of second circle is given as:

$$\left(x - x_n\right)^2 + \left(y - y_n\right)^2 = r_n^{\;2} \quad (17)$$

Then, the point of intersection P (x_p, y_p) of the line joining the target B_i and B_{i+1} and the line joining intersected circles of radii r_m and r_n is the novel point defined as:

$$x_p = \left\{\left(x_m + x_n\right)\left(x_m - x_n\right) + 2*\left(r_n^2 - r_m^2\right)\right\}/2*\left(x_m - x_n\right) \quad (18)$$

$$y_p = \left\{(r_m^2 - r_n^2 + x_n^2 - x_m^2 + y_n^2 - y_m^2) - 2*\left(x_n - x_m\right)x_p\right\}/2*\left(y_n - y_m\right)$$

$$(19)$$

The robust tracking zone is developed by drawing a new circle with diameter $d_o = r_m$ over the line joining the target B_i and B_{i+1} at the novel point where the future position of the target B_{i+n} is localized and tracked inside the intersection of the two beams from the two reference nodes. Figure 4 illustrates the determination of tracking-zone deploying two friendly nodes as references. Once the tracking zone is determined, the two reference nodes and the target node exchange packets which contain the ToD and ToA of each packet. The average of (ToA – ToD) provides the range between the target and any one reference node.

The beam widths adapted by reference nodes A_j and C_k at distance D_j and D_k from the centre of zone having the zone radius r= r_m are Θ_{Aj} and Θ_{Ck} defined by equations (14)- (15).

$$\Theta_{Aj} = 2 \arcsin(r / D_j) \quad (20)$$

$$\Theta_{Ck} = 2 \arcsin(r / D_k) \quad (21)$$

The Euclidean distances and angle of arrivals of reference nodes about the target node are computed as D_{AB}, D_{CB} and $\Box_{AB}$, $\Box_{CB}$ in equations (22)-(25).

$$D_{AB} = c * \sum_{i=1}^{n}(ToA_i^{BA} - ToD_i^{AB})/n \quad (22)$$

$$D_{CB} = c * \sum_{i=1}^{n}(ToA_i^{BC} - ToD_i^{CB})/n \quad (23)$$

$$\theta_{AB} = \sum_{i=1}^{n}(\theta_i^{AB})/n \,(24)\; \theta_{CB} = \sum_{i=1}^{n}(\theta_i^{CB})/n$$
$$(25)$$

The location of target node B(x_{AB}, y_{AB}) from node A is (x_{AB} =D_{AB} Cos $\Box_{AB}$, y_{AB} =D_{AB} Cos $\Box_{AB}$) and B(x_{CB}, y_{CB}) from node A is (x_{CB} =D_{CB} Cos $\Box_{CB}$, y_{CB} =D_{CB} Cos $\Box_{CB}$) respectively. The position trajectory of a target node A moving with velocity 'v' at time 'Δt' is estimated by node B and node C are P_{AB} and P_{CB} as in equations (26) and (27).

$$P_{AB} = v_{target}(x_{AB} + y_{AB})\Delta t = v_{target} * D_{AB}(\cos\theta_{AB} + *\sin\theta_{AB}) * \Delta t$$
$$(26)$$
$$P_{CB} = v_{target}(x_{CB} + y_{CB})\Delta t = v_{target} * D_{CB}(\cos\theta_{CB} + *\sin\theta_{CB}) * \Delta t$$
$$(27)$$

This can be further deployed in mapping the relative PL&T of the malicious node to GPS information in 2D if any reference node happens to have a known GPS data. Furthermore, the use of dynamic PL&T algorithm is supplemented by the use of Koay-Vaman (KV) transform technique to improve the performance of the algorithm in the presence of multi-path fading [12]. It has been shown that by using sample interleaving and error correction, the data can be recovered at very low Bit Error Rate (BER) at $E_b/N_0 < 10$ db.

Dynamic switching of reference nodes in PL&T is the assignment of new friendly reference nodes as per requirement when the existing friendly node becomes no malicious during the periodic authentication. In addition, when the target node goes out of range from the current reference nodes during PL&T operation then another friendly node is switched after ranging and authentication. Dynamic switching overhead is increased when the

velocity of target is comparatively higher than that of reference nodes.

2.3 Modeling the movement of Malicious Targets

We assume that the malicious target node changes its direction randomly. The motion of target node can be represented as follows:

$$x_i(t) = \psi\, V\quad \theta_i \qquad (28)$$

$$\psi_i(t) = F_\psi(t) \qquad (29)$$

where, $x_i(t)$ represents the B_i^{th} position of the target, $\psi_i(t)$ refers the orientation of target's antenna beam, v is the target's active velocity, and $V^{\vee}(\theta_i)$ represents the direction of motion, specified as $V^{\vee}(\theta_i) = \cos(\theta_i)\, x^{\vee} + \sin(\theta_i)\, y^{\vee}$.

The active direction of motion is determined by the angle θ_i, in which a target changes the direction θ_i at any instant time, with probability P_{turn}. The orientation of the antennas is determined in the functional order of $F_\psi(t)$. Deploying Friis transmission, the received power of signals sent by A_j^{th} and C_k^{th} transmitter (neighbors) at B_i^{th} target or receiver node with a power above a certain threshold δ can be expressed in two-dimensions as:

$$Pr_j(x_i,\ \psi_i, x_j)\ \psi() = K\,Pt_j G_{Tj}(\psi_j,\ x_{ij}\ G_{Rj}\ \psi_i\ x_{ji}\ x^2_{ij}) > \delta \qquad (30)$$

$$Pr_k(x_i,\ \psi_i, x_k)\ \psi() = K\,Pt_k G_{Tk}(\psi_k,\ x_{ik}\ G_{Rk}\ \psi_i\ x_{ki}\ x^2_{ik}) > \delta \qquad (31)$$

Regarding A_j^{th} transmitter, Pt_j is the transmission power of the transmitter, $G_{Tj}(\psi_j^{\vee}.x_{ij})$ denotes the gain of the transmitter in the direction to the target or receiver, $G_{Rj}(\psi_i^{\vee}.x_{ji})$ represents the gain of the target or receiver in direction of the transmitter, K is angular diffusion as $K=(\eta^2/24)\ P_{turn}$ where θ_i depends on a step function of width η, and $\psi^{\vee}= \cos(\psi_j)\, x^{\vee} + \sin(\psi_j)\, y^{\vee}$, at $x_{ij}= x_i - x_j$ and so on for k^{th} transmitter.

Pr $(x_{ij}, \psi_{ij}, x_{ik}, \psi_{ik})$ is the received power of signals by the target node which is the sum of the received energy power $Pr_j(x_i, \psi_i, x_j, \psi_j)$ and $Pr_k(x_i, \psi_i, x_k, \psi_k)$ from both tracking nodes.

$$Pr(x_{ij},\ \psi_{ij}, x_{ik},\ \psi_{ik}) = Pr_j(x_i,\ \psi_i, x_j,\ \psi_j) + r_k Pr(x_i,\ \psi_i, x_k,\ \psi_k)$$

$$= K\{\ Pt_j\ G_{Tj}(\psi_j\ x_{ij})\ G_{Rj}\ \psi_i\ x_{ji}\ x^2_{ik}$$

$$+ Pt_k G_{Tk}(\psi_k(x_{ik}\ G_{Rk}\ \psi_i/(x_{ki}\ x^2_{ij}))x^2_{ij}\ x^2_{ik}$$

$$(32)$$

At every broadcasting time instant Δt, the position of the target is updated by a simple Euler method such that $x_i(t+\Delta t) = x_i(t) + v\ V^{\vee}(\theta_i(t))\ \Delta t$. The direction of motion of node $\theta_i(t)$ at each time step with probability P_{turn} is updated by $\theta_i(t + \Delta t)$ which is a random angle between 0 and 2π. Otherwise, $\theta_i(t + \Delta t) = \theta_i(t)$. The estimation of antenna's Beam Direction $\psi_i(t)$ is such that the probability of rotation is P_{rot} for $\psi_i(t + \Delta t)$ as a random angle between 0 and 2π.

$$G_{TR}(\psi_{jk}, x_{jk}, x_i) = G_M(\gamma_{ij}^{TR}) + G_M(\gamma_{ik}^{TR}),$$

$$for\ \psi_j\ x_{ij} < \cos 5\ \gamma_j^{TR})\ and\ \psi_k\ x_{ik} < \cos 5\ \gamma_k^{TR})$$

$$= 1.4\{(2 - \cos(0.5\gamma_{ij}^{TR}) - \cos(0.5\gamma_{ik}^{TR})) / (1 - \cos(0.5\gamma_{ij}^{TR})) (1 - \cos(0.5\gamma_{ik}^{TR}))\}$$

$$(33)$$

$$G_{TR}(\psi_{jk}, x_{jk}, x_i) = G_S(\psi)_j\ x_{ij} + G_S\ \psi_k\ x_{ik}$$

$$for\ \psi_j\ x_{ij} > \cos 5\ \gamma_j^{TR})\ and\ \psi_k\ x_{ik} > \cos 5\ \gamma_k^{TR})$$

$$= 1.4\{(2 - (\psi_k)\ x_{ij}(\ -.\psi_k))x_{ik}(1\ (\ -.\psi_k))x_{ij}(\ -.\psi_k))x_{ik}$$

$$(34)$$

The transmission and receiving gain G_{TR} pair between two tracking nodes and target is computed using γ^{TR} as the angle for maximum gain for the transmitter and receiver as shown in equations (55) and (34).

The states of target and reference nodes can be modeled as time dependent systems. Initially, A_j^{th} and C_k^{th} tracking nodes are in searching 'S' mode for target B_i^{th} in the space. In other words, these two nodes are broadcasting the message, and looking for target in their power range. The 'S' mode is replaced by 'T' as A_j^{th} and C_k^{th} nodes keep tracking target B_i^{th} till it is found inside the range. When the target B_i^{th} is in either 'S' or 'T' mode, the internal clock is coupled with mode by Δt. If the internal clock coupled at mode 'S' marks a time larger than τ, the state of the agent is changed to reset 'R' mode of the clock. If the mode 'R' keeps the clock for a time larger than R_τ, the agent moves back to the 'S' mode. The transition from 'S' to 'T', and from 'R' to 'S' are finite processes.

2.4 Simulation and Performance Evaluation

The simulation platform is set up using the simulation parameters as listed in Table-2. Malicious Detection Rate is higher until the network become denser or crowded. The major reason is that member nodes become closer to each other in highly populated cluster and this may create the similar location information and get mis-detected. In addition, when higher number of new nodes entered into the cluster then cluster could not register all of them simultaneously and unregistered nodes become malicious. The malicious detection rate is 100% for 10 member nodes, vary between 92-100% for 11-20 member nodes, 91-98% for 21-45 member nodes and 89-94% for 46-60 member nodes as shown in Figure 5. Themalicious nodes which do not participate are assumed to be non existing nodes. The friendliness maintenance in PL&T is required which is done by eliminating malicious nodes appeared as reference nodes. This is done by dynamic switching of the malicious reference nodes by friendly nodes. The malicious and friendly nodes participation are equivalent at particular number of participated nodes between 10-20, 30-40 and 45-60 in simulation shown in Figure 6. The major reason is that the co-located nodes have equi-probable conditions in maintaining and violating the location information during hash security based friendliness authentication.

PL&T performance is evaluated in terms of distance over time such that target is moving in random direction at different speed in the range of 10m/s and 40 m/s. The speed is lower only when the target makes the sharp turn along its path and higher along straight path. The tracking zone is developed and ranging is done using adaptive beam forming over the target. When a single location is not pin pointed for a target then the error is equally distributed forboth references to pin point the target, if the error is within the threshold circle of 1 m diameter, otherwise ranging is repeated. The PL&T estimationis performed and the tracking zone is dynamically formed depending upon the target's position. This PL&T error is achieved by the comparison between "true target position" and "PL&T estimatedposition" for a range of distance and time instances. The average PL&T error is 4.16 m for as shown in Figure 7.

TABLE II
SIMULATION PARAMETERS

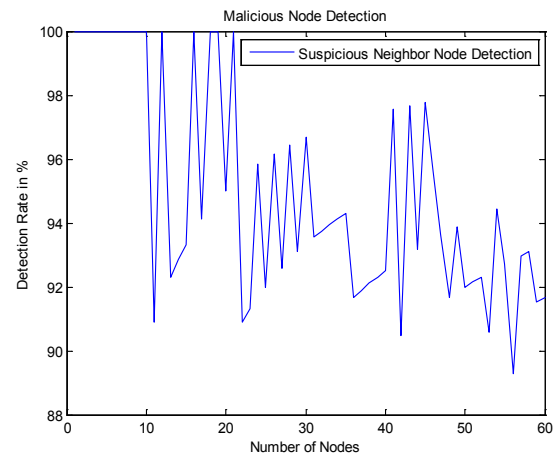| Element	Value
Cluster Area (sq. m)	500X 500
Density of Nodes	60
Directional Antenna Range (m)	40
Channel Frequency (GHz)	2.54
Radiation Efficiency	0.82
Transmitted Power (dbm)	40
Antenna Size (m)	1
No. of Antenna Elements	5

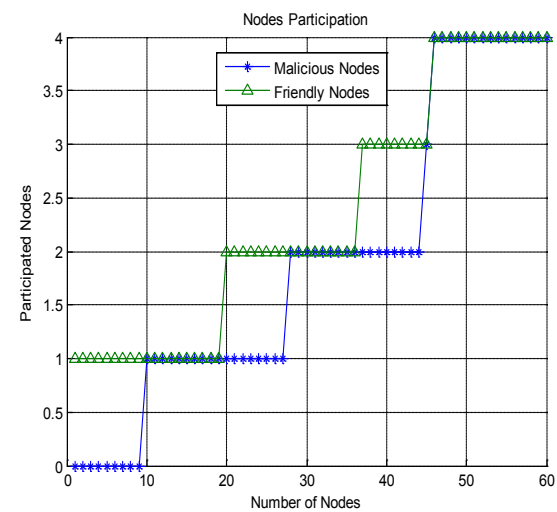Fig. 5 Malicious Node Detection

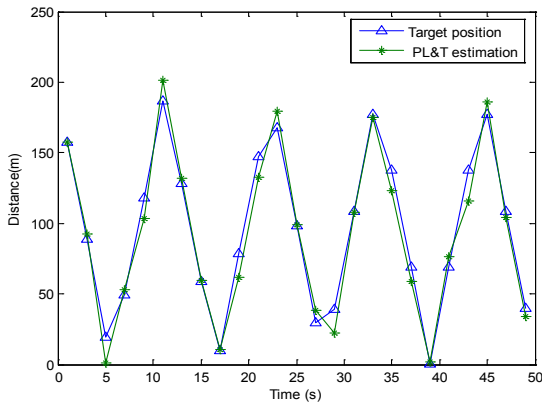Fig. 6 Friendly & Malicious Nodes participation in PL&T

Fig.7 PL&T Estimation

Additionally, the average error of PL&T is demonstrated at different adaptive beam width with random directional movement in Figure 8. The average error goes on increasing with increasing Beam width of tracking nodes over target because higher coverage tracking zone spread the beam energy. The average error percentage is found significantly lower during location tracking in dynamic PL&T with two reference nodes than single reference node even in higher beam width, because of the joint participation of two nodes during narrowed zone finding, adaptive beam forming and average ranging. The minimum average error is 0.04 m at 1 degree beam width and maximum average error is 2.4 m at 60 degree beam width in one reference node using DA. Similarly, the minimum average error is 0.02 m at 1 degree beam width and maximum average error is 1.74 m at 60 degree beam width in the proposed PL&T.
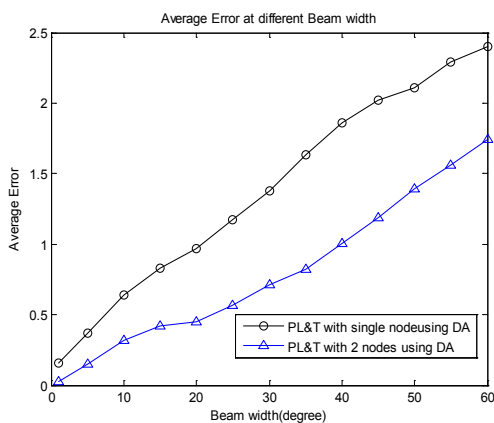

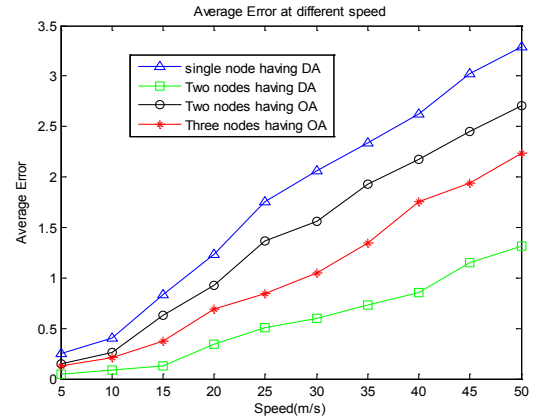Fig. 8 Average error of PL&T over Beam width

Fig. 9   Comparison of different PL&T schemes

The average error of PL&T is demonstrated at different speed with random directional beam width as well as Omni-directional (OA) beam and found that it goes on increasing with increasing speed of target because of multipath fading and Doppler spread. The average error percentage is found highest in the lack of robust coverage and scalable tracking zone in single node using adaptive beam forming DA, than triangulation based PL&T with two nodes having OA, three nodes having OA and the lowest in two nodes having directional antenna for adaptive beam forming based Dynamic PL&T. The minimum average error is 0.05m at 5m/s and maximum average error is 1.35m at 50 m/s in proposed two nodes based PL&T which proves that the proposed PL&T is very efficient as compared to two OA based PL &T and single directional antenna based PL&T as shown in Figure 9.

PL&T simulation shows that the average broadcasting time increases with the increasing probability of changing directions by target because the target always move away in other random direction and it consumes more time to allow the data to be successfully received by the target. Figure 10 shows the average broadcasting time over probability of "changing direction" by the target. This indicates that the beam width of reference nodes plays a vital role specially narrower beam width provides the long range which significantly increases the speed of broadcasting packets and consumes lower broadcasting time. This is sustained as the average broadcasting time is found the most efficient in 15 degree beam width than 30 degree beam width, 45 degree beam width, 60 degree beam width, 90 degree beam width and Omni-directional, even the probability of turning of target is increased.
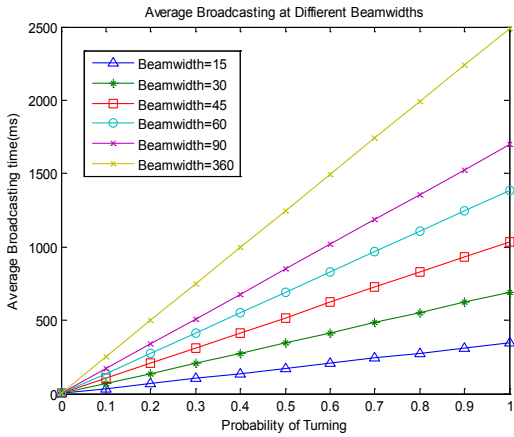
Fig. 10 Average Broadcasting over $P_{turning}$ of target

When the tracking zone is wider, the target can be exactly localized and tracked inside the same zone for higher number of trajectory trials until target does not move away. This increases the tracking efficiency but reduces tracking accuracy as the beam is spread over large coverage. On the contrary, when the zone is smaller, the target falls outside the existing zone and need to update the zone. This reduces the tracking performance as the computational time overhead is accumulated when the zone is frequently updated. In addition, when the zone is narrow the beam width is also narrow and it increases the tracking accuracy as well as data transmission rate. This is the tradeoff between the zone size and tracking accuracy which can be manipulated as the converse relation between the beam width and zone updating time overhead. The increasing zone size yields the increasing beam width which increases the PL&T estimation error but decreases the zonal computational overhead time in time in different experiments and vice-versa.

2.5 Dynamic PL&T using interleaving KV transform under Doppler Spread multipath fading

Since multi-path fading forces the tracking operation to be conducted at low E_b/N_o, it is essential to maintain a bounded BER with an average sustained data transmission rate. Using KV transform, it is possible to interleave discrete samples and allow one out of four discrete samples to be corrected exactly, it is expected that both bit error rate and tracking accuracy improves significantly. The bit error rate is improved using sample interleaving KV transform over without interleaving. Figure 11 shows the tracking accuracy improvement when using KV transform that allows

sample interleaving over that of without interleaving because of correlated bits recovery.
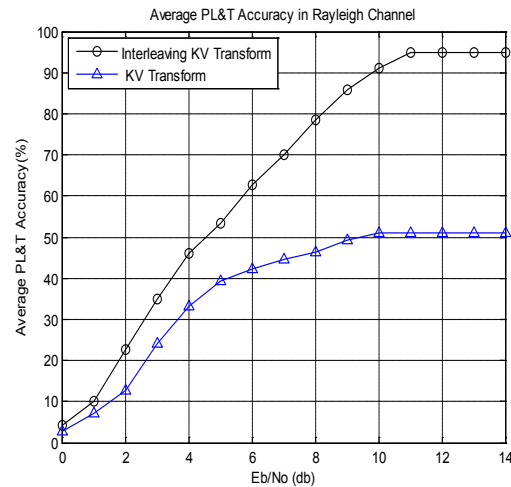

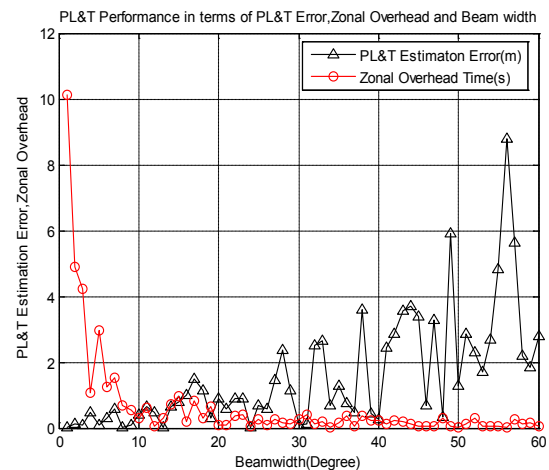Fig.11 Tracking Accuracy using KV Transform

Fig.12 DPL&T in multipath fading(without KV)

Dynamic PL&T has found higher tracking accuracy for bits interleaving KV during data transmission and reception against the multipath interference. For typical wireless channels, the BER is around 10^{-4}. Figure 11 show that using KV transform coding, it is possible to achieve a tracking accuracy of over 90% using 10 db of Eb/No for BER above 10^{-6} and therefore allows the dynamic PL&T algorithm to be very robust under multipath faded channels.

With the increasing beam width, zonal overhead for updating zone decreased but the PL&T estimation error increased as shown in Figure 10 (without KV transform). The zonal overhead is increased for narrow beam width as the zone need to be reconstructed frequently whereas decreased in wide beam width. The estimated PL&T error increased in
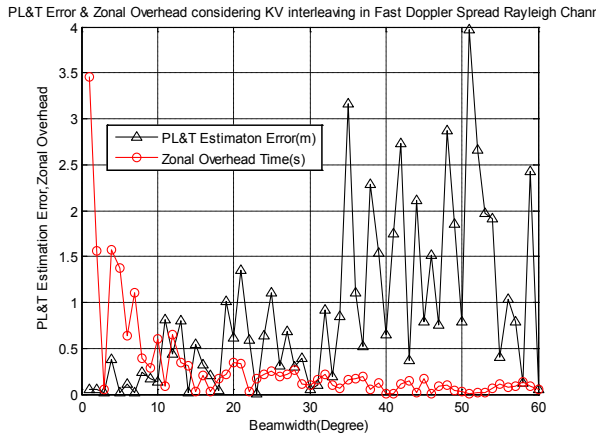
Fig.13 D-PLT in Fast Doppler Rayleigh Channel

Fig.14 D-PLT in Slow Rayleigh Channel

the severe multipath fading channel with the increasing beam width. The PL&T estimated error has frequent jitters because the multipath faded channel model induced the random number of taps among three to ten. From the simulation results shown in Figure 12-14, the critical beam width for Dynamic PL&T is found 10 degree above which the zonal overhead decreases and estimation error increases significantly. The optimum beam width for Dynamic PL&T deploying narrow zone-forming and triangulation using two reference nodes, is 10 degree to optimize the estimation error and zonal overhead.

The Doppler spread spectrum for mobile speed =35m/s, carrier frequency F_c=2.54 GHz, maximum Doppler frequency shift fmax=45Hz and Doppler spectrum function vary from -4 to 4 at Doppler frequency of -44 Hz to 44 Hz. Doppler spread function increases at the higher range of frequencies observed at the output of the channel. PL&T error and zonal overhead is significantly reduced in fast Doppler spread Rayleigh channel than slow Doppler spread Rayleigh channel because the KV interleavingtransform has significantly better bit recovery performance against the deleterious effect in fast fading channel than slow fading channel under severely varying multiple taps. In other words, transmitted bits can be significantly recovered for symbol time (T_s) > coherent time (T_c) and signal bandwidth (B_s) < channel bandwidth (B_D). From simulation results, the average estimated location tacking errordecreased from 4m to 6m and average zonal overhead also decreased from 4 to 8 in fast Doppler spread fading than slow Doppler spread fading as shown in Figure 11 and Figure12. The major reason is that slow fadingchannel has only single realization and error cannot be detected and corrected whereas fastfading allow detection
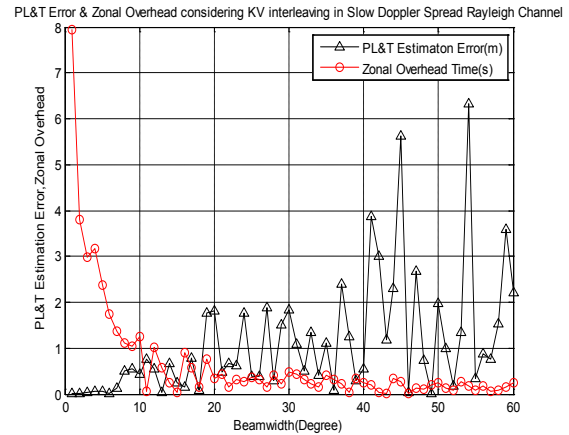
and error correction which leads to the significant tracking accuracy.

3. Conclusion

This paper described specific dynamic PL&T algorithm using the location based hash scheme to detect the malicious and friendly nodes, and friendly nodes track malicious node by adapting beam width over tracking zone. The average PL&T error is found significantly lower in the proposed PL&T scheme than other PL&T schemes. In addition, the optimum beam width for dynamic PL&T is 10 degree to optimize the estimation error and zonal overhead. On the other hand, the performance in terms of tracking accuracy is significantly improved in faded channels when using interleaving KV transform coding and achieves >90% accuracy using 10 db of E_b/N_o. The average PL&T error and zonal overhead are significantly reduced in fast Doppler spread Rayleigh channel than slow Doppler spread Rayleigh channel.

4.References

[1]Shakhakarmi N., Vaman R. D.:Distributed Position Localization and Tracking (DPLT) of

Malicious Nodes in Cluster Based Mobile Ad hoc Networks (MANET), WSEAS Transactions in Communications, ISSN: 1109-2742, Issue 11, Volume 9, November 2010.

[2]Shakhakarmi N.,Vaman R. D.: Real Time Position Location & Tracking (PL&T) usingPrediction Filter and Integrated Zone Finding in OFDM Channel, WSEAS 2012 Transactions in Communications, E-ISSN: 2224-2864, Issue 7, Volume 11 , pp-241-250, July 2012.

[3]Shakhakarmi N.,Vaman R. D.: Integrated Key based Strict Friendliness Verification of Neighbor in MANET, IJCST Jan 22, 2011.

[4] Xiaofeng L., Fletcher W., Ian L., Pietro L., Zhang X.: Location Prediction Algorithm for Directional Communication, Computer Laboratory, University of Cambridge, U.K, Beijing University of Aeronautics and Astronautics Beijing, UK, IWCMC, 2008.

[5] Malhotra N., Krasniewski M., Yang C., Bagchi S., Chappell W. :Location Estimation in Ad-Hoc Networks with Directional Antennas, Purdue University, ICSCS, 2005.

[6] Siuli R., Sanjay C., Somprakash B.,Tetsuro U., Hisato I., Sadao O.: Neighborhood Tracking and Location Estimation of Nodes in Ad hoc Networks Using Directional Antenna: A Testbed Implementation, Proceedings of the WCC, Maui, Hawaii, USA, June 13-16, 2005.

[7] Zhang B., Yu F.: Low-complex energy-efficient localization algorithm for wireless sensor Networks using directional antenna, Department of Integrated Electronics, Shenzhen Institutes of Advanced Technology, IET Commun., 2010, Vol. 4, Iss. 13, pp. 1617–1623.

[8] Yanchao Z., Wei L., Wenjing L.,Yuguang F.: Securing Sensor Networks with Location – Based Keys, IEEE Wireless Communications and Networking Conference, 2005, 1909 - 1914 Vol. 4,13- 17 March 2005.

[9] Huang Z., Shen C: Multibeam Antenna- Based Topology Control with Directional Power Intensity for Ad Hoc Networks, IEEE Trans. Mobile Comput., vol. 5, no. 5, May 2006.

[10] Peruani F., Maiti A., Sadhu S., Chat´e H., Choudhury R., Ganguly N.:ModelingBroadcasting Using Omni-directional and Directional Antenna in Delay Tolerant Networks as an Epidemic Dynamics," IEEE J. Sel. Areas Commun., vol . 28, no. 4, May 2010.

[11] Zhang Z., Iskander M., Yun Z., Madsen A.: Hybrid Smart Antenna System UsingDirectional Elements—Performance Analysis in Flat Rayleigh Fading, IEEE Trans. SignalProces., vol. 51, no. 10, October 2003.

[12]Ramanathan R., Redi J., Santivanez C., Wiggins D., Polit S.: Ad HocNetworking with Directional Antennas: A Complete System Solution, IEEE J. Sel. Areas Commun.,vol .23, no.3, March 2005.